

# COMPRESSIVE IMAGE FUSION

Tao Wan Nishan Canagarajah Alin Achim

Department of Electrical and Electronic Engineering  
University of Bristol, Bristol, BS8 1UB, UK  
{Tao.Wan, Nishan.Canagarajah, Alin.Achim}@bristol.ac.uk

## ABSTRACT

Compressive sensing (CS) has received a lot of interest due to its compression capability and lack of complexity on the sensor side. In this paper, we present a study of three sampling patterns and investigate their performance on CS reconstruction. We then propose a new image fusion algorithm in the compressive domain by using an improved sampling pattern. There are few studies regarding the applicability of CS to image fusion. The main purpose of this work is to explore the properties of compressive measurements through different sampling patterns and their potential use in image fusion. The study demonstrates that CS-based image fusion has a number of perceived advantages in comparison with image fusion in the multiresolution (MR) domain. The simulations show that the proposed CS-based image fusion algorithm provides promising results.

*Index Terms*— compressive sensing, image fusion

## 1. INTRODUCTION AND MOTIVATION

Recent theoretical results in compressive sensing [1, 2] show that sparse or compressible signals can be accurately reconstructed from a small set of incoherent projections. Usually, the number of samples required for reconstructing the original signal can be far fewer than the number of samples if the signal is sampled at the Nyquist rate, thus providing the benefits of reduced storage space and transmission bandwidth due to the phenomenal compression achieved. For this reason CS has been proposed as a viable candidate in many practical applications, such as data compression, wireless communication, sensor networks, compressive imaging, etc. However, there is little literature on CS concerning its application to image fusion. Image fusion is the combination of multiple images into a single fused image that aids human visual perception or subsequent image processing tasks. One method of achieving image fusion is with a multiresolution decomposition scheme [3, 4, 5]. All these methods require knowledge of the original images. A natural question emerges about the possibility of fusing images without acquiring the original input images. One key advantage offered by the CS approach is that samples can be collected without assuming any prior information about the signal being observed, thereby motivating our research on compressive image fusion.

In this paper, we first analyze the impact of different sampling patterns on the compressive sensing reconstruction. For this purpose, three patterns are employed to sample the image in the Fourier domain similar to that of [6]. The image is then recovered via a total variation optimization presented in [1]. The performance of the

Tao Wan was supported by an Overseas Research Students Award (OR-SAS).

sampling patterns is tested on various types of images, especially, on multimodal images, which are used in the proposed CS-based image fusion algorithm. Finally, an image fusion algorithm is presented in the compressive domain using different sampling patterns. The experiments show that our proposed double-star-shaped pattern achieves better reconstruction results as well as fusion results. Due to its universality and simplicity on the hardware side [7], compressive sensing is an attractive scheme for image fusion. CS-based image fusion possesses a number of advantages over conventional image fusion in the multiresolution domain. These are discussed in Section 5.

The remainder of the paper is organized as follows. Section 2 provides background on CS and introduces new sampling patterns with their performance on the CS reconstruction. In Section 3, a conventional image fusion problem in the multiresolution domain is described. A new CS-based image fusion algorithm and simulation results are presented in Section 4 and Section 5, respectively. Finally, conclusions and suggestions for future work are given in Section 6.

## 2. COMPRESSIVE SENSING AND SAMPLING PATTERNS

Compressive sensing enables a sparse or compressible signal to be reconstructed from a small number of non-adaptive linear projections, thus significantly reducing the sampling and computation costs. CS has many promising applications in signal acquisition, compression and medical imaging. In this paper, we investigate its potential application in the image fusion. First, we provide a brief introduction to compressive sensing and explore the impact of different sampling patterns on the CS reconstruction.

### 2.1. Background on Compressive Sensing

Consider a real-valued, finite-length, one-dimensional signal<sup>1</sup>  $\mathbf{x} \in \mathbb{R}^N$  with elements  $x[n], n = 1, 2, \dots, N$ . We say that the signal is  $K$ -sparse if it can be represented as:

$$\mathbf{x} = \Psi\boldsymbol{\theta} \quad (1)$$

where  $\Psi$  is some basis and  $\boldsymbol{\theta}$  is a vector containing only  $K \ll N$  nonzero coefficients.  $\boldsymbol{\theta}$  can be thought of as  $\mathbf{x}$  in domain  $\Psi$ . In CS, we do not measure or encode  $\boldsymbol{\theta}$  directly, rather, we take the compressive measurements:

$$\mathbf{y} = \Phi\mathbf{x} \quad (2)$$

where  $\mathbf{y} \in \mathbb{R}^M$  and  $\Phi$  is an  $M \times N$  matrix representing the measurement process. Although  $M < N$  makes the recovery of the

<sup>1</sup>An image can be vectorised into a long one-dimensional vector.

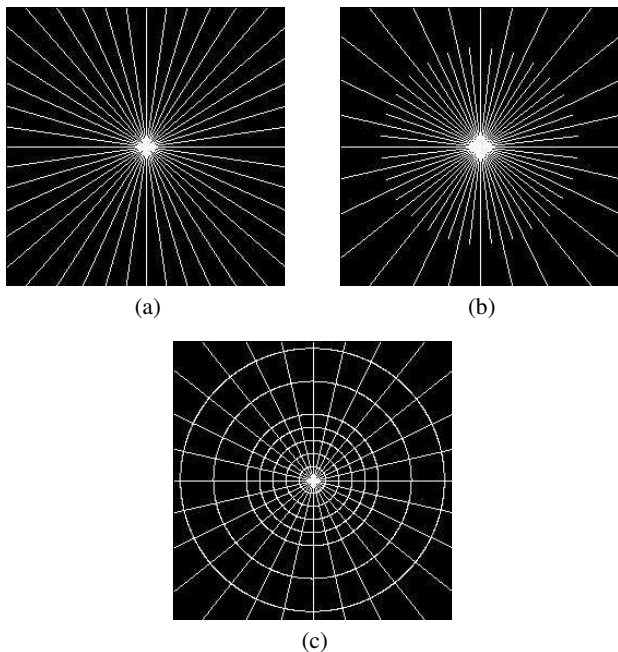


**Fig. 1.** Sampling patterns (a) Star shape. (b) Double-star shape. (c) Star-circle shape.

signal  $\mathbf{x}$  from the measurements  $\mathbf{y}$  ill-posed in general, recent CS experiments show that the recovery is possible and practical by adding assumption of signal sparsity [8].

## 2.2. Sampling Patterns in CS Measurement

From Section 2.1, it is known that compressive measurements  $\mathbf{y}$  are obtained from a nonadaptive linear projection of the signal onto a random  $M \times N$  measurement basis matrix  $\Phi$ . There are different ensembles of CS matrices defined in previous CS literature. For example, in [2], Donoho considered a uniform Spherical ensemble, and Candès et al. used random partial Fourier matrices and showed several interesting properties of this ensemble in CS [1]. Due to the special structure of the Fourier transform underlying the partial Fourier ensemble, the use of such matrices greatly expands the applicability of the CS scheme into large scale data, e.g. 2-D images [8]. For example, a toolbox called *ll-magic* [6] used 2-D fast Fourier transform and the CS matrix  $\Phi$  was constructed by a star-shaped sampling pattern in the 2-D Fourier plane, as shown in Fig. 1(a). The sampling pattern consists of white lines indicating the locations of the frequencies used to compute compressive measurements  $\mathbf{y}$ . Once  $\mathbf{y}$  have been measured, a reconstruction algorithm is employed to recover original signal  $\mathbf{x}$  from the measurements  $\mathbf{y}$ . Therefore, the choice of different sampling patterns will lead to different measurements. There are two issues which need to be addressed: how the sampling patterns affect the reconstruction process, and whether a sampling pattern with superior performance to the star-shaped one can be found.

To investigate these problems, we design two new sampling patterns according to the properties of the 2-D Fourier transform by ensuring that the number of compressive samples remains the same as for the star-shaped one. Due to the fact that the low frequencies

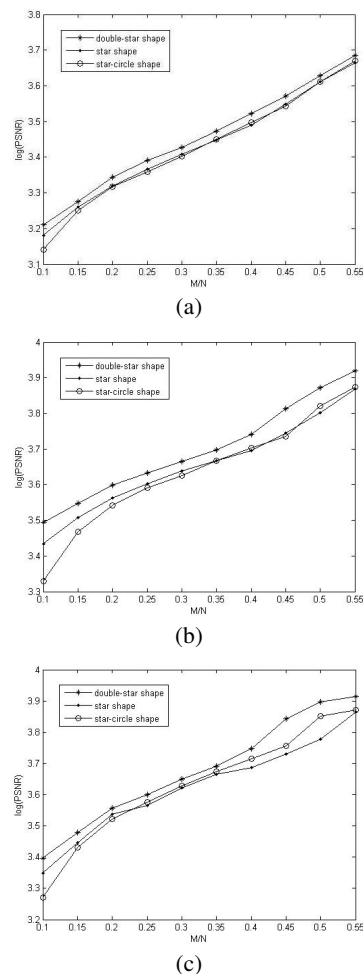


**Fig. 2.** Log values of PSNR for reconstructions of a variety of images. (a) Natural images. (b) IR images. (c) Visible images.

are centered at the origin of the frequency coordinate system and the high frequencies are away from the center. Images usually have lots of low frequency information, so the lines are chosen with higher density sampling at low frequency, like two stars centered at the same origin. We name the pattern “double-star”, shown in Fig. 1(b). Inspired by the Gabor filter which divides the spectrum into slices, we design a pattern with a similar structure which also has higher density sampling at low frequency. The pattern is called “star-circle” shown in Fig. 1(c). By changing the density of lines in the sampling patterns, we can obtain different numbers of measurements.

All the three patterns illustrated in Fig. 1 are tested on various types of images, including natural images [9], infrared (IR) and visible images [10]. These surveillance images are also used in the following image fusion experiments. Fig. 2 presents the peak signal-to-noise ratio (PSNR) of the recovered images for these three sampling patterns. The  $M/N$  on the  $x$ -axis is the rate of the CS measurements over the original signal. The figure shows that better quality images can be obtained by simply taking more measurements because the CS measurement process is progressive. In these three cases, the double-star-shaped pattern yields the best performance for all the

three types of images in terms of the PSNR values. We also notice that the reconstruction process demands less computation time by using the double-star-shaped pattern. This is because that this sampling pattern makes a good balance of choosing the low frequencies and high frequencies in the Fourier domain.

### 3. IMAGE FUSION IN THE MULTIREOLUTION DOMAIN

Multiresolution decompositions (e.g. pyramid, wavelet, linear, etc.) have shown significant advantages in the representation of signals. They capture the signal in a hierarchical manner where each level corresponds to a reduced-resolution approximation. MR methods in image fusion are very important for various reasons. First, MR representations enable one to consider and fuse image features separately at different scales. They also produce large coefficients near edges, thus revealing salient information [11]. Moreover, MR methods offer computational advantages and appear to be robust. In past decades, wavelets have emerged as an effective tool for this problem due to their energy compaction property [3, 4, 5]. In this paper, we address the image fusion problem in the context of wavelet transforms. As our main focus is not on MR image fusion, we choose a simple maximum selection (MS) fusion scheme to fuse the input images at the pixel level. MS is a widely used fusion rule which considers the maximum absolute values of the wavelet coefficients from the source images as the fused coefficients.

The wavelet-based image fusion algorithm consists of two main components. First, the detailed wavelet coefficients are composed using the MS fusion rule:

$$D_F = D_M \quad \text{with} \quad M = \arg \max_{i=1, \dots, I} (|D_i|) \quad (3)$$

where  $D_F$  are the composite coefficients,  $D_M$  is the maximum absolute value of the input wavelet coefficients, and  $I$  is the total number of the source images.

Because of their different physical meaning, the approximation and detail images are usually treated by the combination algorithm in different ways. Then a popular way to construct the fused approximation image  $A_F$  is:

$$A_F = \frac{1}{I} \sum_{i=1}^I (A_i) \quad (4)$$

The fused image is obtained by taking an inverse wavelet transform. As we can see, an image fusion approach based on wavelets requires to manipulate detailed coefficients and approximation images, while in the compressive domain, it only considers the compressive measurements.

### 4. IMAGE FUSION IN THE COMPRESSIVE DOMAIN

In this section, we formulate an image fusion algorithm that uses compressive measurements to fuse multiple images into a single representation. Recent theoretical results show if the signal is sparse or nearly sparse in some basis, then with high probability, the measurements essentially encode the salient information in the signal. Further, the unknown signal can be estimated from these compressive measurements to within a controllable mean-squared error [1, 2]. In this sense, we can apply a similar fusion schemes to that used in the wavelet domain in the compressive domain, so the difference is that image fusion is performed on the compressive

measurements rather than on the wavelet coefficients. The basic steps are described in Algorithm 1.

---

#### Algorithm 1 Compressive image fusion algorithm

---

1. Take the compressive measurements  $Y_i, i = 1, \dots, I$  for the  $i^{th}$  input image using the double-star-shaped sampling pattern.
  2. Calculate the fused measurements using the formula:  $Y_F = Y_M$  with  $M = \arg \max_{i=1, \dots, I} (|Y_i|)$ .
  3. Reconstruct the fused image from the composite measurements  $Y_F$  via the total variation optimization method [1].
- 

## 5. SIMULATION RESULTS AND DISCUSSIONS

An objective evaluation criterion is applied to compare fusion results obtained using different sampling patterns. A quality metric which does not require a ground-truth was proposed by Piella and Heijmans [12] in which the important edge information is taken into account to evaluate the relative amount of salient information conveyed in the fused image. We use their defined criterion to evaluate the fusion performance. In Fig. 3 we present some results of the proposed image fusion algorithm applied to three pairs of images. There is a clear performance improvement by using the double-star-shaped sampling pattern over the other two patterns. We also note that by using nearly 50% fewer compressive measurements than reconstructed pixels, we can achieve almost the same fusion results as using the entire set of pixels. Fig. 4(c) and 4(d) illustrate two fused images using half and all Fourier coefficients to obtain compressive measurements, respectively. As can be seen, there is no perceivable difference between these two images.

CS-based image fusion has a number of advantages over conventional image fusion algorithms. It offers computational and storage savings by using a compressive sensing technique. Compressive measurements are progressive in the sense that larger numbers of measurements will lead to higher quality reconstructed images. Image fusion can be performed without acquiring the observed signals. Additionally, the recently proposed compressive imaging system [7], which relies on a single photon detector, enables imaging at new wavelengths inaccessible or prohibitively expensive using current focal plane imaging arrays. This new development of the imaging system has made it promising to exploit the CS-based image fusion in a practical use. This will significantly reduce the hardware cost, meanwhile expand image fusion in modern military and civilian imaging applications in a cheaper and more efficient way. However, the compressive measurements lose spatial information due to the CS measurement process. Therefore, traditional image fusion rules operating on local knowledge cannot be applied to compressive image fusion.

## 6. CONCLUSIONS AND FUTURE WORK

In this paper we have presented a study on sampling patterns and their impact on the CS reconstruction performance of compressive sensing for 2-D images. We found that the designed double-star-shaped pattern outperforms the other two patterns by means of better recovered image quality and less computational complexity. We also investigated the image fusion application in the compressive domain which appears to have not been explored thus far. There are a

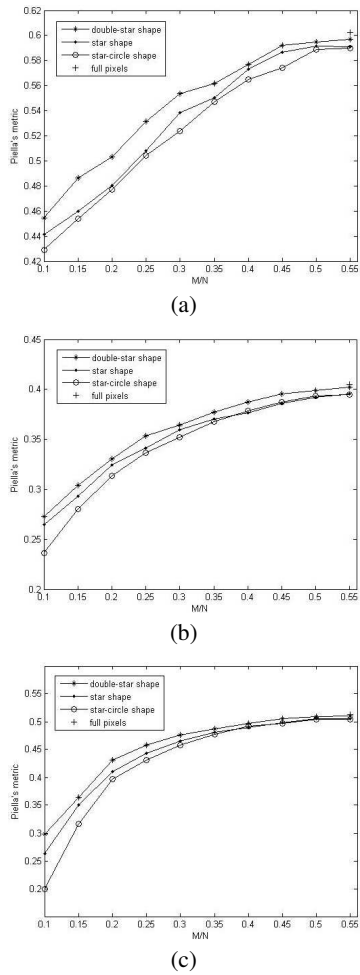


**Fig. 3.** Piella's metric results using different sampling patterns for different images. (a) “Kayak” images. (b) “UN Camp” images. (c) Medical images.

number of advantages of combining the compressive sensing technique and image fusion application. However, a CS-based fusion algorithm cannot use window-based fusion schemes due to a lack of spatial information in the compressive measurements. By studying the statistical properties of the compressive measurements, a new and higher-complexity fusion rule needs to be developed in the future.

## 7. REFERENCES

- [1] E. Candès, J. Romberg, and T. Tao, “Robust uncertainty principles: Exact signal reconstruction from highly incomplete frequency information,” *IEEE Trans. Inform. Theory*, vol. 56, no. 2, pp. 489–509, 2006.
- [2] David L. Donoho, “Compressed sensing,” *IEEE Trans. Inform. Theory*, vol. 52, no. 4, pp. 1289–1306, Apr. 2006.
- [3] G. Piella, “A general framework for multiresolution image fusion: from pixels to regions,” *Information Fusion*, vol. 4, pp. 259–280, 2003.

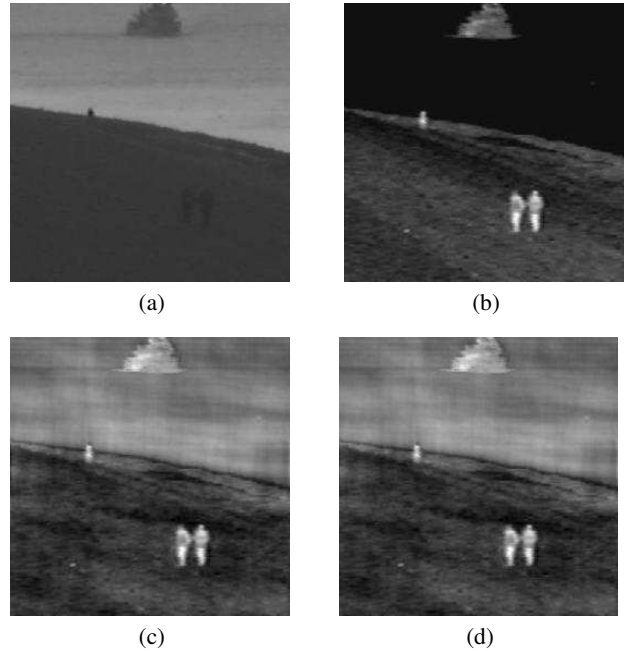


**Fig. 4.** Fusion results using the double-star-shaped sampling pattern. (a)  $256 \times 256$  original “Kayak” visible image. (b)  $256 \times 256$  original “Kayak” IR image. (c) Fused image recovered from  $M = 32768$  compressive measurements ( $M/N = 0.50$ ). (d) Fused image using all Fourier coefficients ( $N = 65536$ ).

- [4] Tao Wan, Nishan Canagarajah, and Alin Achim, “Region-based multisensor image fusion using generalized Gaussian distribution,” in *Int. Workshop on Nonlinear Sign. and Image Process.*, Sep. 2007.
- [5] Tao Wan, Nishan Canagarajah, and Alin Achim, “Context enhancement through image fusion: A multiresolution approach based on convolution of cauchy distributions,” in *Proc. IEEE Conf. Acoustics, Speech and Signal Process. (to appear)*, Mar. 2008.
- [6] Emmanuel Candès and Justin Romberg, *l1-magic: Recovery of sparse signal via convex programming*, code package available at <http://www.l1-magic.org>.
- [7] M. B. Wakin, J. N. Laska, M. F. Duarte, D. Baron, S. Sarvotham, D. Takhar, K. F. Kelly, and R. G. Baraniuk, “An architecture for compressive imaging,” in *Proc. of the IEEE Int. Conf. Image Process.*, Oct. 2006, pp. 1273–1276.
- [8] Yaakov Tsaig and David L. Donoho, “Extensions of compressed sensing,” *Signal Process.*, vol. 86, pp. 549–571, May. 2005.
- [9] *The Berkeley Segmentation Dataset Benchmark*, University of California, Berkeley, CA, available at <http://www.eecs.berkeley.edu/Research/Projects/CS/vision/grouping/segbench/>, Jul. 2003.
- [10] *The Online Resource for Research in Image Fusion*, available at <http://www.imagefusion.org/>.
- [11] D. Marr, *Vision*, W. H. Freeman, New York, 1982.
- [12] Gemma Piella and Henk Heijmans, “A new quality metric for image fusion,” in *Proc. IEEE Conf. Image Process.*, 2003, vol. 2, pp. 173–176.